Surface plasmon waves generated by nanogrooves through spectral interference

Qiaoqiang Gan,[1] Yongkang Gao,[1] Qing Wang,[2] Lin Zhu,[3] and Filbert Bartoli[1,*]
[1]*Center for Optical Technologies, Electrical and Computer Engineering Department, Lehigh University, Bethlehem, Pennsylvania 18015, USA*
[2]*Nano-optoelectronics Laboratory, Institute of Semiconductors, Chinese Academy of Sciences, P.O. Box 912, Beijing 100083, China*
[3]*Department of Electrical and Computer Engineering, Center for Optical Materials Science and Engineering Technologies, Clemson University, Clemson, South Carolina 29634, USA*
(Received 19 January 2010; published 25 February 2010)

A pure surface plasmon polariton (SPP) model predicted that the SPP excitation in a slit-groove structure at metallodielectric interfaces exhibits an intricate dependence on the groove width P. Lalanne *et al.* [Phys. Rev. Lett. **95**, 263902 (2005); Nat. Phys. **2**, 551 (2006)]. In this paper, we present a simple far-field experiment to test and validate this interesting theoretical prediction. The measurement results clearly demonstrate the predicted functional dependence of the SPP coupling efficiency on groove width, in good agreement with the SPP picture.

DOI: 10.1103/PhysRevB.81.085443 PACS number(s): 73.20.Mf, 42.25.Bs, 78.68.+m

I. INTRODUCTION

Since Ebbesen's report on extraordinary optical transmission through plasmonic hole arrays was published in 1998,[1] there has been considerable growth in plasmonics research, fueled in part by rapid advances in nanofabrication and nanocharacterization techniques. However, because of the multiple processes that occur in the nanoaperture geometries studied,[2,3] an in-depth interpretation of the experimental results has proven difficult. To better understand surface plasmon polariton (SPP) mediated interactions between optical nano-objects at metallodielectric interfaces, researchers have conducted numerous theoretical and experimental studies of the physics of simple nanostructures, e.g., single or double slits,[4] grooves,[5] or apertures.[6] But even for the simplest single slit-groove structure, some initial debate arose regarding the physical mechanisms underlying these interactions.[7–10] Recent theoretical progress in this area is described in several recent reviews,[11–13] and researchers generally agree that both SPP modes and transient surface waves[14] (also called quasicylindrical waves[5] or creeping waves[8]) play important roles in interactions between optical nano-objects. However, in recent years, theoretical analyses[15–18] have significantly outpaced experimental investigations,[19–25] and some remarkable theoretical predictions have not yet been experimentally realized. For example, the SPP model predicts that the SPP excitation probabilities in simple slit-groove structures exhibit an intricate dependence on slit width[15,16] or groove width.[8] In this article, we design a simple far-field experiment and present a systematic experimental investigation of these slit-groove nanostructures to test this interesting theoretical prediction. Experimental validation of theoretical models is critical if they are to be employed in the design of future nanoplasmonic devices. The measurement results clearly demonstrate the predicted functional dependence of the SPP coupling efficiency on groove width, in good agreement with the SPP picture.[8]

II. FAR-FILED EXPERIMENT TO OBSERVE THE SPP-MEDIATED SPECTRAL INTERFERENCE

We first discuss the simple far-field experiment employed to observe the SPP-mediated spectral interference. Surface-wave interferometers consisting of single slit–single groove pairs with varying slit-groove separation distance and groove width were fabricated by FIB milling (FEI Dual-Beam system 235). These structures were patterned on a Ag layer evaporated onto flat fused silica microscope slides (Fisherbrand). The optical transmission measurements were performed using an Olympus X81 inverted microscope, in which a white light beam from a 100 W Halogen lamp was focused at normal incidence onto the sample surface (air side) through the microscope condenser with a linear polarizer. The transmitted light was collected by a X40 microscope objective with a numerical aperture of 0.6, coupled into a multimode fiber bundle that was connected to a fiber-based compact spectrometer (Ocean Optics USB 4000). A charge coupled device (CCD) camera was employed to align the position of the slit-groove pairs. An illustration of the groove or slit geometry is shown in Fig. 1. To optimize the spectral interference patterns, the peak intensity of the white light beam was aligned with the groove. A diaphragm in the condenser was employed to control the intensity of the light beam illuminating the slit (see Fig. 1). A similar setup was employed to study the group velocity of SPP modes on flat metal surfaces, except that the white light beam illuminated the sample from the substrate side.[26] This measurement approach has the advantage of being simpler and easier to re-

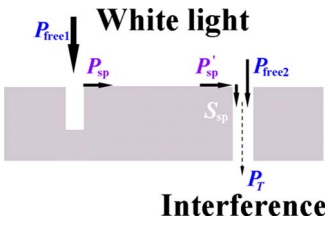

FIG. 1. (Color online) Sketch of the groove or slit geometry.

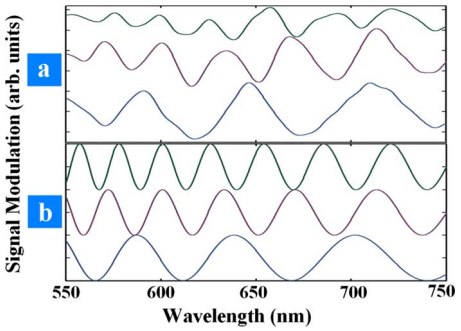

FIG. 2. (Color online) Spectral interference launched by slit-groove pairs on a Ag film. (a) Measurement results for the slit-groove separation distance L of 5.24 μm (lower), 8.39 μm (center), and 10.24 μm (upper). (b) Theoretical plots of the interference signal modulations with L of 5.24 μm (lower), 8.39 μm (center), and 10.24 μm (upper). The refractive index of the dielectric on top of the metal is numerically set to 1.175.

peat than experiments involving more demanding alignment, data processing,[4,7,14,19–25] or instrumentation (e.g., the near-field scanning microscope[19,20] or leakage radiation microscope[6,21–23]). For example, experiments in Refs. 7 and 14 were performed at a single wavelength and required an angle-tunable Goniometer equipped with a lock-in amplifier to extract the SPP-assisted spatial interference information. Each data point was extracted from a slit-groove pair, indicating that a large number of samples were required to measure a single interference pattern. In contrast, the experiment reported in our work does not involve such complicated or time consuming measurements. A white light source illuminates the sample and the measurement provides a clear interference pattern over a wide spectral region all at once.

Now we discuss the experimentally observed SPP-mediated spectral interference using this set up. SPP modes launched at the groove propagate to the slit (see Fig. 1) and will interfere with the free-space light. For an incident plane wave with a unit power per slit-opening area, the far-field transmitted intensity is given by the expression

$$I_t(\lambda) = E_{\text{free}}^2 + E_{\text{spp}}^2 + 2E_{\text{free}}E_{\text{spp}} \times \cos\left(\frac{2\pi L}{\lambda}\sqrt{\frac{\varepsilon_m'(\lambda)n^2}{\varepsilon_m'(\lambda)+n^2}} + \varphi_0\right), \quad (1)$$

where a cosine term represents the interference. Here E_{free} and E_{spp} are the electrical fields of the free-space light and SPP modes, respectively. L is the slit-groove separation distance, n is the refractive index of the dielectric material on top of the metal surface, and φ_0 is an additional phase shift.[4] The first set of samples was fabricated on a 300-nm-thick layer of Ag. The length and width of the slit or groove are 20 μm and 200 nm, respectively. The slit-groove separation distances are 5.24, 8.39, and 10.64 μm. The polarization of the incident light is either parallel (TE) or perpendicular (TM) to the long axis of the slit or groove. Spectral interference patterns are clearly observed under TM illumination, as shown in Fig. 2(a), suggesting SPPs propagating along the metal surface lie at the heart of the observed phenomena. In this plot, the low-frequency background and high-frequency noise have been numerically filtered using a fast Fourier transform (using a low-frequency cutoff at $\sim$2.896 μm^{-1} and a high-frequency cutoff at $\sim$217.196 μm^{-1}). One can see that the spectral interference pattern can be tuned by changing the separation distance between the slit and groove. However, when we employ empirically derived optical constants of Ag (Ref. 27) (see also the supplementary material of Ref. 28 for details of the data fitting) and Eq. (1) to plot the spectral interference modulation, we find that the calculated number of periods is lower than that observed experimentally and that the wavelengths of the SPP modes derived from the measured data are smaller than those predicted for the Ag/air surface. It should be noted that in the theoretical calculation, φ_0 is assumed to be a constant for all the wavelengths. In a recent report of near-field SPP characterization at UV wavelengths, we reported a similar discrepancy in the derived wavelength.[29] This observation is consistent with results previously reported in Ref. 7 and raised as a points concern in Refs. 8–10. To explore this further, one should consider the potential effect of surface roughness and a possible contamination layer of Ag_2S (or a mixture of Ag_2O/AgO) on top of the Ag surface[8,30] on the effective refractive index. If one arbitrarily assumes a refractive index of 1.175 for the dielectric material on top of the metal, the theoretical interference patterns agree well with the measured results [see Fig. 2(b)]. Besides the obvious effect of a contamination layer on the refractive index, it was believed that surface roughness could also affect the damping properties of SPP modes.[31] To clearly address this question, detailed surface characterization is required, including surface element analysis and measurement of the thickness of this contamination layer and its corresponding surface roughness. It was noted in Ref. 10 (b) that the effect of the contamination layer could be isolated by performing a similar measurement on a Au film. However, effects of the surface roughness were not considered as an important factor in recent works, e.g., Refs. 7–10. Recent measurements in our laboratory demonstrated that the surface roughness can also have a significant effect on the properties of SPP modes on metallodielectric interfaces.[32] In addition, a vertical incidence is also important. However, these issues are beyond the scope of the present work. The key issue which will be addressed in this work is the experimental confirmation of the remarkable predictions of the theoretical SPP model proposed by Refs. 8, 15, and 16. As emphasized in Ref. 8, the SPP excitation probabilities exhibit an intricate dependence on slit width or groove width, which has not been fully realized experimentally.

III. DEPENDENCE OF THE SPECTRAL INTERFERENCE PATTERN ON GROOVE WIDTH

We first employ an analytical model to calculate the dependence of the spectral interference pattern on groove width. According to Ref. 8, the SPP coefficient S for coupling into the fundamental slit mode is given by

$$S = t_0 + \alpha\beta W + \alpha^2 W r_m V^2\left(\frac{t_0 + \alpha\beta W}{1 - r_m r_0 V^2}\right), \quad (2)$$

where $W=\exp(ik_{sp}L)$, k_{sp} is the SPP propagation constant at the Ag/dielectric interface, and V is the phase factor associ-

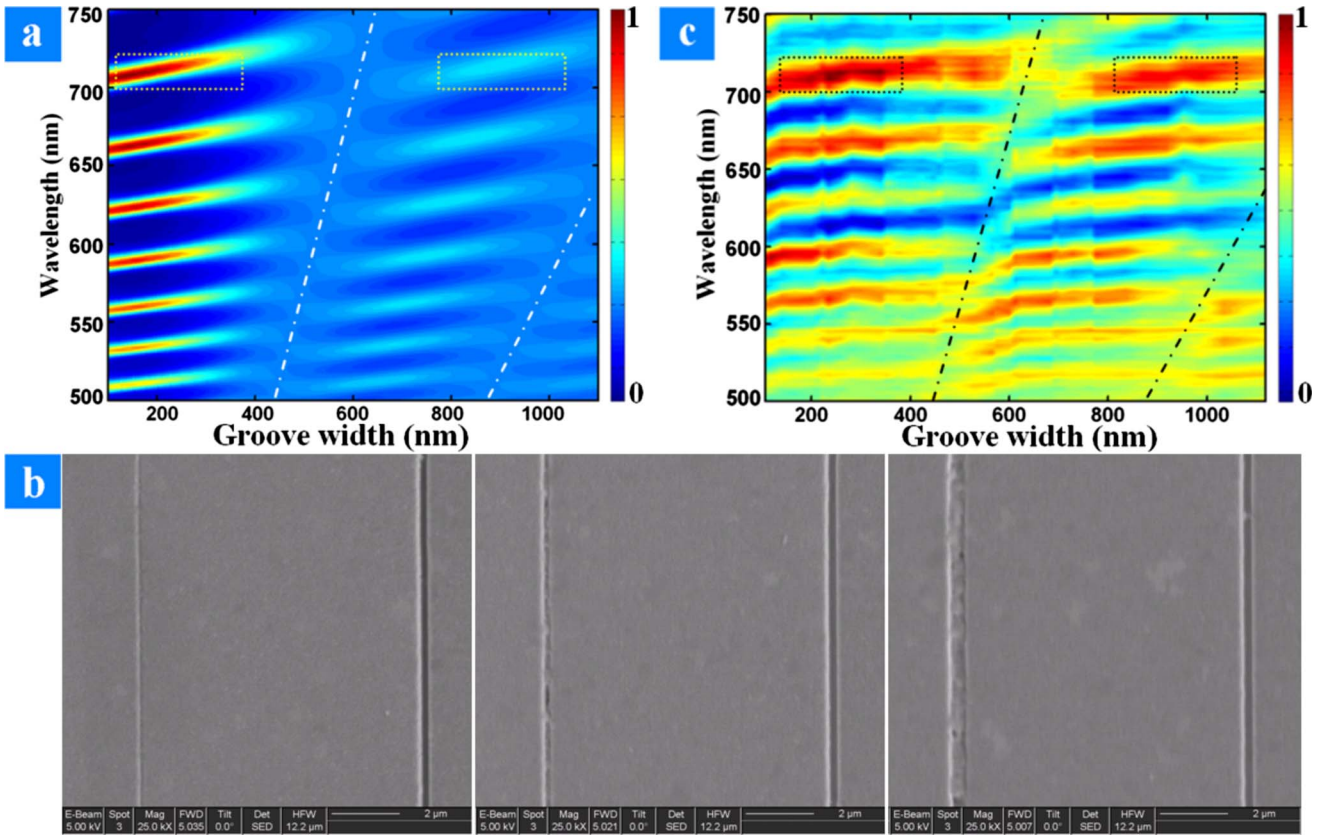

FIG. 3. (Color online) Dependence between the spectral interference pattern and the groove width. (a) Numerical simulation using Eq. (2): the slit-groove separation and the groove depth are set to 8.39 μm and 150 nm, respectively. In this simulation, we assumed that there is a contamination layer of Ag_2S on top of the Ag surface. The equivalent refractive index of the material on top is numerically set to 1.175. (b) Scanning electron microscope images of three slit-groove structures with the groove width of 106, 165, and 471 nm, respectively. (c) Measurement results: the widths of the grooves are 106, 118, 141, 165, 200, 212, 222, 235, 259, 282, 341, 353, 376, 400, 424, 447, 459, 471, 529, 565, 575, 600, 612, 624, 682, 694, 706, 729, 765, 776, 835, 871, 918, 953, 988, 1035, and 1118 nm. In (a) and (c), we first normalized S (λ, groove width) to $S0$ (λ, groove width) assuming no grooves. Then we normalized the values of $S/S0$ again.

ated with light bouncing in the groove. As discussed in Ref. 8, the modal coupling coefficients, α, β, t_0, r_m, and r_0 are known quantities that couple the incident plane wave, the slit or groove fundamental modes, and the SPP at the Ag/air interface. We used Eq. (2) and followed the numerical procedure developed in Refs. 8, 15, and 16 to determine the functional dependence of the normalized coupled power $|S|^2/|S0|^2$ on the groove width and wavelength. The normalized calculated results for $|S|^2/|S0|^2$ are shown in Fig. 3(a). In this simulation, the slit-groove separation and the groove depth are set to 8.39 μm and 150 nm, respectively, which are identical to the parameters of the samples we fabricated. One can observe obvious peaks and valleys as a function of varying groove width. As a guide to the eye, the positions of the valleys are illustrated by the white lines in Fig. 3(a); the first cutoff appears at a width of approximately $w_c=0.92\lambda$ (Ref. 8) and the second one appears at about $w_c=1.84\lambda$.

Next we present a systematic experimental investigation of slit-groove nanostructures to validate this SPP model. Thirty seven groove-slit pairs were fabricated on a 300-nm-thick layer of Ag. The width of the slit was fixed at approximately 520 nm, and the width of the groove finely tuned from 106 to 1118 nm [see Fig. 3(b), detailed width data is listed in the caption to Fig. 3]. The depth of the groove is roughly 150 nm. According to Ref. 5, when the slit-groove distance is greater than 4–5 times of the incident wavelength, the contribution from quasicylindrical (or transient surface) waves is negligible. To safely distinguish SPP waves from transient surface waves generated by the nanogroove, the slit-groove separation distance was fixed at approximately 8.39 μm, which is ten times greater than all wavelengths employed in the measurements. Figure 3(c) presents the measured interference patterns as a function of groove width and wavelength. Definite cutoff groove widths (illustrated by the black lines) can be observed and are found to be in a reasonably good agreement with the theoretical predictions shown in Fig. 3(a). While precise peak positions are difficult to determine due to noise and experimental uncertainty, we nevertheless find good correlation between the experimental data and theoretical predictions. For example, the experimental peaks in the interference patterns for the 700–730 nm wavelength range are observed at groove widths of 212–259 nm (corresponding to $0.29\lambda-0.37\lambda$), and at 918–953 nm [see the data in Fig. 3(c)]. This is in reasonable agreement with the theoretical calculations, which predict the first peak to appear at $w\approx 0.23\lambda$.[5,8] We believe that this observation strongly validates the predictive capabilities of the SPP model.

IV. EXTRACTION OF THE SPP-GENERATION EFFICIENCY

Finally we discuss the extraction of the SPP-generation efficiency as a function of groove width from the experimental data. While the SPP-generation efficiency can, in principle, be extracted at any wavelength, here we consider the data at a wavelength of 710 nm as an example to demonstrate the data analysis. The optical path is shown in Fig. 1. Since the light beams illuminating the slit and the groove are generally nonuniform, the expression for the interference is more somewhat complicated than that given in Eq. (1). Here we employ the averaged power density $I_{\text{free}}(\lambda)$. Consequently, the power of the free space light incident on a groove of width w and length of D is $P_{\text{free }1}=I_{\text{free }1}(\lambda)wD$. Similarly, the power illuminating the 520-nm-wide slit is $P_{\text{free }2}=I_{\text{free }2}(\lambda)\times 520\ \text{nm}\times D$. The power coupled into the SPP mode traveling toward the slit is given by $P_{sp}(\lambda,w)=1/2e_{\text{spp}}(\lambda,w)\times I_{\text{free }1}(\lambda)wD$, where the $e_{\text{spp}}(\lambda,w)$ is the SPP-generation efficiency.[15] The factor of 1/2 in this expression accounts for the fact that SPP modes propagating away from the slit will not interfere with the free space light. As the SPP mode propagates toward the slit, the power decays to $P'_{sp}(\lambda,w)=P_{sp}(\lambda,w)\exp(-2k''_{sp}L)$, where k''_{sp} is the imaginary part of the wave vector of the SPP modes and L is the slit-groove distance. The SPP modes will next be coupled into the slit modes with a power of $S_{sp}=1/2e'_{\text{spp}}(\lambda,520\ \text{nm})\times P'_{sp}(\lambda,w)$, where e'_{spp} is the coupling efficiency from the SPP modes to the free space light at the slit. Consequently, the transmitted power is given by

$$P_T(\lambda,w)=S_{sp}(\lambda,w)+P_{\text{free }2}(\lambda,520\ \text{nm})T+2[S_{sp}(\lambda,w)P_{\text{free }2}(\lambda,520\ \text{nm})T]^{1/2}\cos\varphi, \tag{3}$$

where T is the transmission coefficient through the slit, and the normalized power is given by

$$\frac{P_T(\lambda,w)}{[P_{\text{free }2}(\lambda,520\ \text{nm})T]}=\frac{S_{sp}(\lambda,w)}{P_{\text{free }2}(\lambda,520\ \text{nm})T}+1+2\left[\frac{S_{sp}(\lambda,w)}{P_{\text{free }2}(\lambda,520\ \text{nm})T}\right]^{1/2}\cos\varphi. \tag{4}$$

Here

$$\frac{S_{sp}(\lambda,w)}{P_{\text{free }2}(\lambda,520\ \text{nm})}=\frac{1}{4}e'_{\text{spp}}(\lambda,520\ \text{nm})e_{\text{spp}}(\lambda,w)\exp(-2k''_{sp}L)\frac{I_{\text{free }1}(\lambda)}{I_{\text{free }2}(\lambda)}\frac{w}{520\ \text{nm}}.$$

Equation (4) can be solved to extract the SPP-generation efficiency, e_{spp}. The value of the phase term was determined numerically ($\varphi\approx 88.845$ rad) by fitting Eq. (1) to the measured spectral interference pattern. The transmission coefficient through the 520-nm-wide slit was calculated by numerical finite-difference time-domain (FDTD) simulations to be $T\approx 0.33$, and $k''_{sp}(\lambda:710\ \text{nm})\approx 0.003498\ \mu\text{m}^{-1}$ was determined from published optical data.[27] The slit-groove distance (L) is set to 8.39 μm, and $e'_{\text{spp}}(\lambda:710\ \text{nm},\ w:520\ \text{nm})$ was determined to be 0.03364 using the semianalytical model.[15] We assume that $I_{\text{free }1}(\lambda)/I_{\text{free }2}(\lambda)=100$. Using these parameters and Eq. (4), we extracted the SPP-generation efficiency, e_{spp}, which are shown by the dots in Fig. 4. The semianalytical model proposed by Ref. 15 was employed to calculate the efficiencies as a function of the groove width (see the solid line in Fig. 4). One can see that the extracted values of e_{spp} agree well with the model.

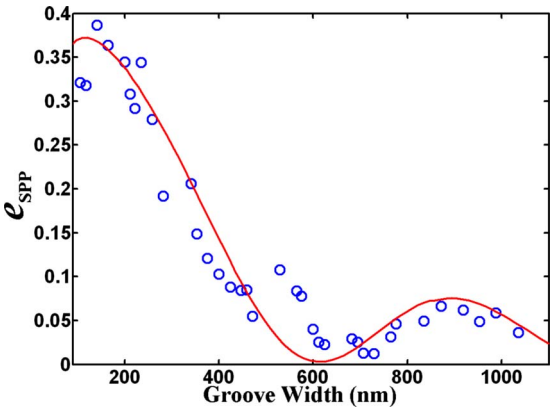

FIG. 4. (Color online) Extraction of the SPP-generation efficiency from the measurement data at the wavelength of 710 nm. Dots-extraction result of the SPP-generation efficiency; solid curve-simulation plot based on the semianalytical model (see Fig. 3 in Ref. 15).

V. CONCLUSION

The spectral interference introduced by the interaction between a nanogroove-slit pair was directly observed, and the strength of the interference pattern found to vary strongly with groove width. The SPP-generation efficiency was also extracted from the experimental data, which agree well with the predictions of the semianalytical SPP model.[8,15] These observations help to develop a better understanding of the physics of the optical interaction between nano-objects and should be useful in the design and optimization of various plasmonic devices, such as compact single plasmonic sources, switches, or modulators.[25]

ACKNOWLEDGMENTS

The authors would like to acknowledge significant assistance in the simulation from P. Lalanne and the support of this research by NSF (Award No. ECCS-0901324).

*fjb205@lehigh.edu

[1] T. W. Ebbesen, H. J. Lezec, H. F. Ghaemi, T. Thio, and P. A. Wolff, Nature (London) **391**, 667 (1998).
[2] W. L. Barnes, A. Dereux, and T. W. Ebbesen, Nature (London) **424**, 824 (2003).
[3] C. Genet and T. W. Ebbesen, Nature (London) **445**, 39 (2007).
[4] H. F. Schouten, N. Kuzmin, G. Dubois, T. D. Visser, G. Gbur, P. F. Alkemade, H. Blok, G. W. 't Hooft, D. Lenstra, and E. R. Eliel, Phys. Rev. Lett. **94**, 053901 (2005).
[5] X. Y. Yang, H. T. Liu, and P. Lalanne, Phys. Rev. Lett. **102**, 153903 (2009).
[6] A. Baudrion, F. Leon-Perez, O. Mahboub, A. Hohenau, H. Ditlbacher, F. J. Garcia-Vidal, J. Dintinger, T. W. Ebbesen, L. Martin-Moreno, and J. R. Krenn, Opt. Express **16**, 3420 (2008).
[7] G. Gay, O. Alloschery, B. Viaris De Lesegno, C. O'Dwyer, J. Weiner, and H. Lezec, Nat. Phys. **2**, 262 (2006).
[8] P. Lalanne and J. P. Hugonin, Nat. Phys. **2**, 551 (2006).
[9] F. J. Garcia-Vidal, S. G. Rodrigo, and L. Martin-Moreno, Nat. Phys. **2**, 790 (2006); J. Weiner and H. Lezec, *ibid.* **2**, 791 (2006).
[10] G. Gay, O. Alloschery, J. Weiner, H. Lezec, C. O'Dwyer, M. Sukharev, and T. Seideman, Nat. Phys. **2**, 792 (2006); P. Lalanne, J. P. Hugonin, M. Besbes, and P. Bienstman, *ibid.* **2**, 792 (2006).
[11] F. J. García de Abajo, Rev. Mod. Phys. **79**, 1267 (2007).
[12] J. Weiner, Rep. Prog. Phys. **72**, 064401 (2009).
[13] P. Lalanne, J. P. Hugonin, H. T. Liu, and B. Wang, Surf. Sci. Rep. **64**, 453 (2009).
[14] F. Kalkum, G. Gay, O. Alloschery, J. Weiner, H. Lezec, Y. Xie, and M. Mansuripur, Opt. Express **15**, 2613 (2007).
[15] P. Lalanne, J. P. Hugonin, and J. C. Rodier, Phys. Rev. Lett. **95**, 263902 (2005).
[16] P. Lalanne, J. P. Hugonin, and J. C. Rodier, J. Opt. Soc. Am. B **23**, 1608 (2006).
[17] H. Liu and P. Lalanne, Nature (London) **452**, 728 (2008).
[18] H. Liu, P. Lalanne, X. Yang, and J. P. Hugonin, IEEE J. Sel. Top. Quantum Electron. **14**, 1522 (2008).
[19] H. W. Kihm, G. K. Lee, D. S. Kim, J. H. Kang, and P. Q. Han, Appl. Phys. Lett. **92**, 051115 (2008).
[20] B. Wang, L. Aigouy, E. Bourhis, J. Gierak, J. P. Hugonin, and P. Lalanne, Appl. Phys. Lett. **94**, 011114 (2009).
[21] A. Drezet, A. Hohenau, A. L. Stepanov, H. Ditlbacher, B. Steinberger, N. Galler, F. R. Aussenegg, A. Leitner, and J. R. Krenn, Appl. Phys. Lett. **89**, 091117 (2006).
[22] A. Drezet, A. Hohenau, D. Koller, A. Stepanov, H. Ditlbacher, B. Steinberger, F. R. Aussenegg, A. Leitner, and J. R. Krenn, Mater. Sci. Eng., B **149**, 220 (2008).
[23] J.-Y. Laluet, A. Drezet, C. Genet, and T. W. Ebbesen, New J. Phys. **10**, 105014 (2008).
[24] S. Ravets, J. C. Rodier, B. Ea Kim, J. P. Hugonin, L. Jacubowiez, and P. Lalanne, J. Opt. Soc. Am. B **26**, B28 (2009).
[25] D. Pacifici, H. J. Lezec, and H. A. Atwater, Nat. Photonics **1**, 402 (2007).
[26] V. V. Temnov, U. Woggon, J. Dintinger, E. Devaux, and T. W. Ebbesen, Opt. Lett. **32**, 1235 (2007).
[27] E. D. Palik, *Handbook of Optical Constants of Solids* (Academic, Orlando, 1985), Vol. 1.
[28] Q. Gan, Y. J. Ding, and F. J. Bartoli, Phys. Rev. Lett. **102**, 056801 (2009).
[29] Q. Gan, L. Zhou, V. Dierolf, and F. Bartoli, Opt. Lett. **34**, 1324 (2009).
[30] P. W. Wilson, J. Vac. Sci. Technol. A **6**, 2386 (1988).
[31] H. Raether, *Surface Plasmons on Smooth and Rough Surfaces and on Gratings, Springer Tracts in Modern Physics* (Springer-Verlag, Berlin, 1988), Vol. 111.
[32] Q. Gan, Y. Gao, S. Jiang, F. Bartoli (unpublished).